THE JOURNAL OF BIOLOGICAL CHEMISTRY
Vol. 274, No. 11, Issue of March 12, pp. 6911–6919, 1999

Printed in U.S.A.

Characterization of the Interaction between the Herpes Simplex Virus Type I Fc Receptor and Immunoglobulin G*

(Received for publication, October 27, 1998)

Tara L. Chapman‡, Il You§, Ian M. Joseph§, Pamela J. Bjorkman‡¶, Sherie L. Morrison‖, and Malini Raghavan§**

From the ‡Division of Biology 156-29 and the ¶Howard Hughes Medical Institute, California Institute of Technology, Pasadena, California 91125, the §Department of Microbiology and Immunology, University of Michigan Medical School Ann Arbor, Michigan 48109, and the ‖Department of Microbiology, Immunology, and Molecular Genetics, UCLA, Los Angeles, California 90095

Herpes simplex virus type I (HSV-1) virions and HSV-1-infected cells bind to human immunoglobulin G (hIgG) via its Fc region. A complex of two surface glycoproteins encoded by HSV-1, gE and gI, is responsible for Fc binding. We have co-expressed soluble truncated forms of gE and gI in Chinese hamster ovary cells. Soluble gE-gI complexes can be purified from transfected cell supernatants using a purification scheme that is based upon the Fc receptor function of gE-gI. Using gel filtration and analytical ultracentrifugation, we determined that soluble gE-gI is a heterodimer composed of one molecule of gE and one molecule of gI and that gE-gI heterodimers bind hIgG with a 1:1 stoichiometry. Biosensor-based studies of the binding of wild type or mutant IgG proteins to soluble gE-gI indicate that histidine 435 at the C_H2-C_H3 domain interface of IgG is a critical residue for IgG binding to gE-gI. We observe many similarities between the characteristics of IgG binding by gE-gI and by rheumatoid factors and bacterial Fc receptors such as *Staphylococcus aureus* protein A. These observations support a model for the origin of some rheumatoid factors, in which they represent anti-idiotypic antibodies directed against antibodies to bacterial and viral Fc receptors.

The expression of viral proteins that counter immune responses of the host is well documented. Viral factors have been identified that can potentially inhibit or modify the antiviral effects of antibodies, complement proteins, cytokines, and cytotoxic T cells (1). Characterization of viral proteins that interact with specific components of the immune system is likely to provide insights into immune mechanisms involved in host-virus interactions and into the molecular basis of viral persistence in the presence of a functional immune system. *Herpesvirus*es, in particular, have evolved multiple mechanisms for interfering with humoral as well as cell-mediated immune responses (reviewed in Refs. 2 and 3). The present studies focus upon the herpes simplex virus type I-encoded Fc receptor (FcR),[1] a protein complex that has been suggested to interfere with antibody-mediated viral clearance (4). HSV-1 virions, as well as cells infected with HSV-1, bind to immunoglobulins of the IgG subclass via the Fc region (5). The glycoprotein gE of HSV-1 was identified as the IgG-binding polypeptide of HSV-1 (6, 7). It was subsequently shown that gE associates with a second viral glycoprotein, gI (8, 9), and that cells transfected with genes encoding both gE and gI have enhanced IgG binding activity compared with cells transfected with gE alone (10–12). Both gE and gI are type I transmembrane proteins, with an N-terminal extracellular portion, a single transmembrane domain, and a C-terminal cytoplasmic domain. Homologous glycoproteins encoded by other α-herpesviruses, including pseudorabies virus (PRV) (13) and varicella zoster virus (14), have been shown to possess species-specific FcR activity.

HSV-1-infected cells acquire low levels of FcR activity immediately upon exposure to virus (in the absence of viral gene expression), presumably by the transfer of virion gE-gI to the cell surface during viral entry (7). The HSV FcR may thus be particularly significant for protection of virally infected cells from early immune destruction (2). Recent *in vivo* studies demonstrated that passively transferred anti-HSV IgG greatly reduced viral titers and disease severity in mice infected with a mutant HSV-1 that lacked FcR activity. By contrast, anti-HSV IgG was ineffective in reducing viral titers and disease severity in mice infected with wild type virus with intact FcR activity (15). These observations indicate that the HSV-1 FcR activity facilitates evasion of antibody-mediated viral clearance *in vivo*.

Several means of evading antibody-mediated immune responses could arise from the Fc binding function of gE-gI (16–18). Binding of nonimmune IgG by gE-gI present on HSV-1 virions can inhibit virus neutralization by anti-viral antibodies (19). Engagement of the Fc portion of anti-HSV antibodies can protect virally infected cells from antibody-dependent cell-mediated cytotoxicity (ADCC) (20) as well as complement-mediated lysis (21). Inhibition of ADCC has been suggested to occur by a phenomenon called antibody bipolar bridging (21), a mechanism whereby antibodies bound via their Fab ends to HSV-1 glycoproteins on surface membranes of infected cells would simultaneously interact with the viral Fc receptors of the same infected cell. By engaging the Fc domain, the HSV-1 FcR could interfere with recognition by FcγRs on immune effector cells. Antibody bipolar bridging has also been suggested to facilitate antiviral antibody-induced patching, capping, and extrusion of

* This work was supported by a grant from the American Heart Association (to M. R.), the University of Michigan Multipurpose Arthritis and Musculoskeletal Diseases Center (to M. R.), and a National Defense Science and Engineering Predoctoral Fellowship (to T. L. C.). The costs of publication of this article were defrayed in part by the payment of page charges. This article must therefore be hereby marked "*advertisement*" in accordance with 18 U.S.C. Section 1734 solely to indicate this fact.

** To whom correspondence should be addressed. Tel.: 734-647-7752; Fax: 734-764-3562; E-mail: malinir@umich.edu.

[1] The abbreviations used are: FcR, Fc receptor; FcγR, Fcγ receptor; PRV, pseudorabies virus; ADCC, antibody-dependent cell-mediated cytotoxicity; PCR, polymerase chain reaction; CHO, Chinese hamster ovary; FACS, fluorescence-activated cell sorting; FITC, fluorescein isothiocyanate; hIgG, human IgG; PAGE, polyacrylamide gel electrophoresis; RF, rheumatoid factor(s); HSV, herpes simplex virus; HSV-1, HSV, type 1.

viral glycoproteins from the surface of cells infected with PRV (13). Antibody-induced shedding of viral glycoproteins may represent a strategy for rendering virally infected cells refractory to antiviral antibodies and for inhibiting the presentation of viral antigens via class II major histocompatibility complex molecules.

A second function attributed to gE-gI is that of facilitating cell-to-cell spread of virus. Recent studies suggest that gE and gI are required for transneuronal transport of PRV from the retina to the visual centers of rats (22), for cell-to-cell spread of PRV, and for full virulence of PRV (23). Furthermore, studies with mutant HSV-1 virions indicate that gE and gI of HSV-1 facilitate cell-to-cell spread of virus *in vivo* and viral spread across junctions of cultured cells (24–26). It has been proposed that the cell-to-cell spread-promoting functions of gE-gI are unrelated to the Fc binding activity and that the HSV-1-encoded gE-gI glycoproteins and the analogous proteins of other α-herpesviruses may interact with other ligands, enabling viral transport across cells (24, 25). Such ligands remain to be identified.

To better understand the mechanisms by which IgG binding by gE-gI facilitates immune evasion, we initiated a molecular characterization of IgG binding by gE-gI. We expressed soluble forms of gE and gI and showed that the glycoproteins assemble into a stable heterodimer. The soluble receptor heterodimer binds to human IgG (hIgG) with relatively high affinity and can be purified to homogeneity using an hIgG-based affinity matrix. We determined a 1:1 binding stoichiometry for the gE-gI·IgG complex, and also determined that a histidine residue at the C_H2-C_H3 domain interface is a critical determinant of IgG binding specificity. The implications of the gE-gI binding site on IgG and the gE-gI·IgG complex stoichiometry are discussed.

EXPERIMENTAL PROCEDURES

Construction and Expression of Soluble gE, gI, and gE-gI—Molecular cloning manipulations were performed by standard protocols (27). PCR was used to insert a 5′ *Xho*I site, a 3′ *Not*I site, and a stop codon after the codon corresponding to amino acid 399 of the gE gene and amino acid 246 of the gI gene (the *Hin*dIII fragment containing the gE gene and the *Bam*HI fragment containing the gI gene of HSV strain KOS was kindly provided by H. Ghiasi, Cedar Sinai Medical Center). Our numbering scheme starts with the first residue of the mature protein, which is designated residue 1, and all other residues are numbered sequentially (see "N-Terminal Sequencing and Mass Spectrometric Analysis of Purified gE-gI"). The gE PCR product was cloned into pCRII (Invitrogen), and the gI PCR product was cloned into pBSIISK$^+$ (Stratagene). Both sequences were verified. The modified gE and gI genes were excised using *Xho*I and *Not*I enzymes and individually subcloned into the unique *Xho*I and *Not*I sites of separate PBJ5-GS expression vectors (28). PBJ5-GS carries the glutamine synthetase gene as a selectable marker and as a means of gene amplification in the presence of the drug methionine sulfoximine, a system developed by Celltech (29). Expression vectors carrying gE, gI, or both gE and gI were transfected into CHO cells using a Lipofectin procedure (Life Technologies, Inc.). Cells resistant to 100 μM methionine sulfoximine were selected according to the protocol established by Celltech, modification of which has been previously described (28). Transfected CHO cells were maintained in glutamine-free α-minimal essential medium (Irvine Scientific) supplemented with 5% dialyzed fetal bovine serum (Life Technologies), 100 μM methionine sulfoximine (Sigma), penicillin (100 units/ml), and streptomycin (100 μg/ml). Cells secreting gE, gI, or both gE and gI were identified by immunoprecipitation of supernatants of cells metabolically labeled with [^{35}S]methionine and [^{35}S]cysteine (see below) by using either an antibody against gE (1108 (Goodwin Institute) or Fd172 (30) (kindly provided by Subbu Chatterjee) or an antibody against gI (Fd69 (31), kindly provided by Subbu Chatterjee) Clones were considered positive if immunoprecipitation yielded a protein of approximately 56 kDa corresponding to gE or a protein of approximately 43.5 kDa corresponding to gI. The identity of each protein was verified using N-terminal sequencing (see below).

^{35}S Metabolic Labeling—gE-, gI-, and gE-gI-transfected CHO cell lines derived from colonies were expanded into 12-well trays, grown to confluence, and incubated for 5 h in 1.0 ml of methionine- and cysteine-free medium (Life Technologies) plus 1% dialyzed fetal bovine serum including 5 μCi of a [^{35}S]methionine and [^{35}S]cysteine (ICN) mixture. Supernatants were clarified by a 5-min spin in a microcentrifuge, and either anti-gE or anti-gI antibodies were added. Immunoprecipitations were carried out by standard methods (32) with protein G-bearing Sepharose beads (Amersham Pharmacia Biotech). Samples were boiled in SDS-polyacrylamide gel electrophoresis (SDS-PAGE) running buffer and loaded onto 15% polyacrylamide gels, which were fixed, dried, and exposed to a PhosphorImager screen (Molecular Dynamics, Inc., Sunnyvale, CA). The image was then developed with a Molecular Dynamics 425E PhosphorImager scanner.

Co-Expression of Full-length gE and gI—PCR was used to insert a 5′ *Xho*I site and a 3′ *Not*I site into the genes encoding gE and gI. The PCR products were sequenced and subsequently individually subcloned into the unique *Xho*I and *Not*I sites of separate PBJ5-GS expression vectors. The two constructs were co-transfected into CHO cells, and cells resistant to 100 μM methionine sulfoximine were selected. Cells expressing both gE and gI were sorted using fluorescence activated cell sorting (FACS) analysis with FITC-labeled hIgG. Individual clones from the sort were amplified and subsequently shown to express both gE and gI by FACS analysis with 1108 or Fd69 as the primary antibodies and a goat anti-mouse IgG as the secondary antibody. Sorting and analysis were performed on a Coulter Epics Elite flow cytometer.

Purification of Soluble gE-gI Heterodimers—gE-gI-secreting CHO cell lines were grown to confluence in 50 10-cm plates and introduced into a hollow bioreactor device (Cell Pharm I; Unisyn Fibertec, San Diego, CA) in serum-free medium, and supernatants were collected daily. Soluble gE-gI heterodimers were purified from supernatants on either a human Fc or hIgG affinity column. The human Fc column was prepared by coupling 20 mg of human Fc (Jackson ImmunoResearch Laboratories, Inc.) to cyanogen bromide-treated Sepharose 4B (Amersham Pharmacia Biotech) at approximately 10 mg of protein/ml of resin according to the protocol of the manufacturer. The hIgG column was prepared similarly using 70 mg of hIgG (Sigma). Supernatants were passed over the affinity column, which was then washed with 50 column volumes of a solution consisting of 50 mM Tris (pH 7.4), 0.1% NaN_3, and 1 mM EDTA. Bound gE-gI was eluted from the column with 50 mM diethylamine (pH 11.5) into tubes containing 1.0 M Tris (pH 7.4). gE-gI heterodimers were further purified using a Superdex 200 HR 10/30 fast protein liquid chromatography (FPLC) filtration column. Approximately 10 mg of gE-gI heterodimers were recovered per liter of transfected cell supernatants.

N-terminal Sequencing and Mass Spectrometric Analysis of Purified gE-gI—N-terminal sequencing was performed on 2.5 μg of purified, soluble gE-gI in a phosphate buffer dried onto a polyvinylidene difluoride membrane and inserted into an Applied Biosystems model 476A sequencer reaction cartridge. Two sequences were isolated from the gE-gI sample: the sequence GTPKTSWRR, corresponding to the first 9 amino acids of mature gE (33), and the sequence LVVRGPTVS, corresponding to the first 9 amino acids of mature gI (33). The molecular masses of gE and that of gI were determined by matrix-assisted, laser desorption, time-of-flight mass spectrometry with a PerSeptive biosystems (Farmington, MA) ELITE mass spectrometer.

CD Analyses—An AVIV 62A DS spectropolarimeter equipped with a thermoelectric cell holder was used for CD measurements. Wavelength scans and thermal denaturation curves were obtained from samples containing 10 μM protein in 5 mM phosphate at pH 7 by using a 0.1-mm path length cell for wavelength scans and a 1-mm path length cell for thermal denaturation measurements. The heat-induced unfolding of gE-gI was monitored by recording the CD signal at 223 nm, while the sample temperature was raised from 25 to 80 °C at a rate of approximately 0.7 °C/min. The transition midpoint (T_m) for unfolding was determined by taking the maximum of a plot of $d\theta/dT$ *versus* T (where θ is ellipticity) after averaging the data with a moving window of 5 points.

Gel Filtration Analyses of gE-gI·hIgG Stoichiometry—Protein concentrations were determined spectrophotometrically at 280 nm using the following extinction coefficients: gE-gI, 88816 M^{-1} cm^{-1}; hIgG, 202,500 M^{-1} cm^{-1}. The extinction coefficient for the gE-gI heterodimer was calculated from the amino acid sequences as described (34), and the extinction coefficient for hIgG is known (32). A_{280} measurements for a fixed amount of each protein were then compared in 6 M guanidine HCl and aqueous solutions, and the extinction coefficients were adjusted as necessary. For determining the gE-gI·hIgG stoichiometry, various molar ratios from 1:3 (300 pmol of gE-gI:900 pmol of hIgG) to 3:1 (900 pmol of gE-gI:300 pmol of hIgG) of gE-gI and hIgG were incubated for 30 min at room temperature in 20 mM Tris, pH 7.4, 150 mM NaCl, 0.05% NaN_3

in a total volume of 100 μl. Samples were injected onto a Superose 6B FPLC column (Amersham Pharmacia Biotech) and eluted with the same buffer at 0.5 ml/min. The composition of each fraction was analyzed by SDS-PAGE (data not shown).

Equilibrium Analytical Ultracentrifugation—Sedimentation equilibrium was performed with a Beckman Optima XL-A analytical ultracentrifuge, using data analysis software provided by the manufacturer. Experiments were performed using 0.6 mg/ml gE-gI at both 4 and 20 °C at a rotor speed of 10,000 rpm, with equilibrium times of at least 36 h. Molecular masses were determined by nonlinear least square fit of the equilibrium gradient, absorbance *versus* radius (Fig. 3), using the model of single ideal species, and a partial specific volume, 0.69, calculated from the amino acid composition and the carbohydrate content (35).

Equilibrium Column Chromatography—The equilibrium column chromatography method of Hummel and Dreyer (36) was used to observe the interaction between gE-gI and hIgG. A Superdex 200 PC 3.2/30 gel filtration column of 2.4 ml was connected to an Amersham Pharmacia Biotech μ Precision pump system. Absorbance of the eluant was monitored at 280 nm with an Amersham Pharmacia Biotech μ Peak monitor. The column was equilibrated with five different concentrations of purified hIgG (Sigma): 250 nM, 500 nM, 1 μM, 2.5 μM, and 5 μM each in 20 mM Tris, pH 7.4, 150 mM NaCl. At each concentration, four 20-μl injections in the appropriate column equilibration buffer (including the relevant concentration of hIgG) were performed. These four injections included gE-gI at a concentration equal to that of the IgG in the column buffer plus no additional hIgG or hIgG at a concentration equal to 1, 2, or 3 times that of the IgG concentration contained in the column buffer. Binding experiments were done at 20 °C with a flow rate of 100 μl/min.

Biosensor Studies—Biosensor studies were performed on a Biacore 2000 instrument. Purified gE-gI was diluted in 10 mM acetate buffer, pH 4.1, for amine-based coupling to a Biacore chip. Immobilization was accomplished by initial activation of the sensor chip with 0.2 M *N*-ethyl-*N*′-(dimethylaminopropyl)-carbodiimide and 0.05 M *N*-hydroxysuccinimide. The *N*-hydroxysuccinimide-ester was then reacted with gE-gI using the manual injection mode to allow for better control of immobilization levels. Typically, an immobilization level of 200–300 response units was used for kinetic analyses described in Table I. The remaining unreacted ester groups were inactivated by 1 M ethanolamine (pH 8.5). Different concentrations of the chimeric IgG molecules were injected over the immobilized gE-gI surface, as well as a control protein surface (murine IgG). A citrate buffer, pH 3.5, was used for regeneration of the surface between sequential injections. Sensorgrams obtained for IgG binding to the control surface were subtracted from those obtained for IgG binding to the gE-gI surface. The BIAevaluation version 3.0 software package was used for kinetic analysis. Kinetic constants were derived by simultaneous fitting to the association and dissociation phases of the subtracted sensorgrams and global fitting to all curves in a working set (Fig. 5). A working set consisted of injections of four or five different concentrations of a hIgG construct over a surface containing immobilized gE-gI. S.D. values are reported from experiments performed in duplicate or triplicate on different sensor chips (Table I). In all cases, a 1:1 binding model was used for curve fitting.

The expression of chimeric hIgG molecules was described previously (37, 38). These molecules are composed of a murine anti-dansyl V_H domain fused to the constant domains (C_H1 through C_H3) of hIgG4. An expression vector containing cDNA encoding the hybrid chain was co-transfected into a non-Ig-producing mouse myeloma line along with an expression vector containing cDNA encoding a chimeric K light chain (composed of a murine anti-dansyl V_K region fused to the human C_K region). Site-directed mutations were introduced into the chimeric heavy chain gene to make the hIgG4H435R mutant and the hIgG3R435H mutant. The hIgG3-hIgG4 chimeras were generated by exon shuffling as described previously (38).

Determination of K_D Values by Cell Binding Assays—Chimeric hIgG4 was iodinated to a specific activity of 16.1 μCi/μg using the chloramine-T method. CHO cell lines expressing full-length gE and gI were grown to confluence in tissue culture plates. Cells were detached by incubation with phosphate-buffered saline (pH 7.5), 5 mM EDTA for 20–30 min and collected in binding buffer at pH 7.0 (Hanks' balanced salt solution, 10 mM HEPES, 0.25% bovine serum albumin). The cells were pelleted, washed once with binding buffer (pH 7.0), and resuspended in binding buffer (pH 7.0). Cells (1×10^6) were mixed in duplicate or triplicate assays with labeled hIgG4, different concentrations of unlabeled hIgG4, and binding buffer (pH 7.0) to a total volume of 0.5 ml. The samples were incubated for 2 h at room temperature. After completion of the incubations, cells were pelleted for 5 min at 14,000 rpm in an Eppendorf microcentrifuge, the supernatants were aspirated, and 1.0 ml of cold binding buffer was added. After removal of the supernatants by aspiration, the tubes were placed in vials, and the levels of radioactivity were determined using a Beckman Gamma 5500 counter. Nonspecific binding was determined by a similar treatment of wild type CHO cells. The binding data were analyzed using Scatchard plots. Assays were performed in triplicate, and the average of the two most similar readings was used to compute the concentration of bound IgG.

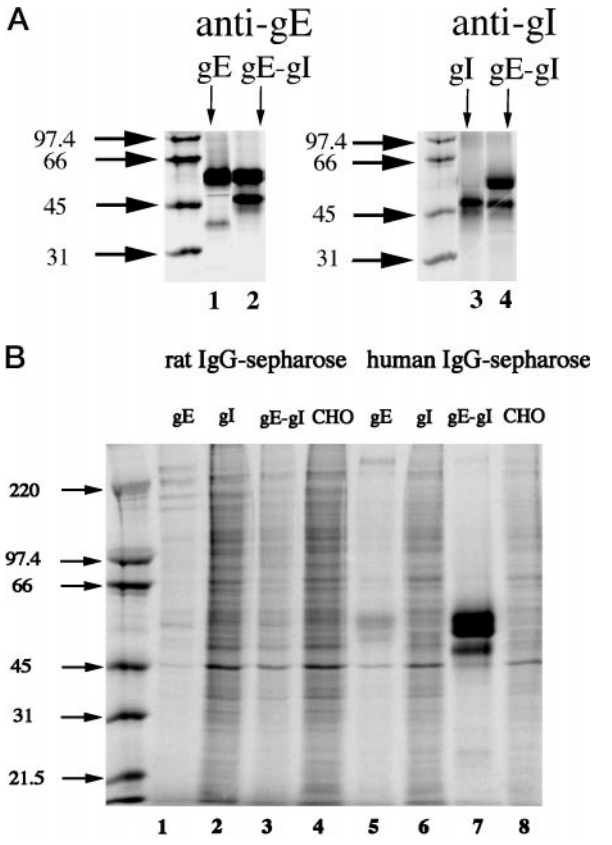

FIG. 1. **Soluble gE and gI assemble into a stable complex.** Cells producing gE, gI, or both gE and gI or nontransfected CHO cells were labeled with [^{35}S]methionine/cysteine, and cell supernatants were analyzed. *A*, SDS-PAGE (10%) analysis of protein isolated from supernatants of ^{35}S-labeled cells producing gE, gI, or gE-gI using antibodies against either gE (*lanes 1* and *2*) or gI (*lanes 3* and *4*). *B*, SDS-PAGE (10%) analysis of gE, gI, and gE-gI binding to either Sepharose-immobilized rat IgG (*lanes 1–4*) or hIgG (*lanes 5–8*).

RESULTS

Co-Expression of Truncated gE and gI Results in Assembly of a Stable Heterodimer—We constructed soluble versions of both gE and gI by truncating each of the genes prior to their predicted transmembrane regions (following the codons for amino acid 399 of mature gE and amino acid 246 of mature gI). The modified genes were co-transfected into CHO cells. Transfected cells were screened by immunoprecipitating supernatants from metabolically labeled cells with antibodies against either gE or gI (Fig. 1*A*). SDS-PAGE analysis of immunoprecipitated protein from gE-gI positive clones revealed two bands with apparent molecular masses of 56 and 43.5 kDa using either the anti-gE or anti-gI antibody. The calculated molecular mass of truncated gE is 42 kDa, and that of gI is 26 kDa; however, both proteins are glycosylated (two potential *N*-linked glycosylation sites in the sequence of gE and three potential sites in the sequence of gI) and would be expected to migrate with a higher apparent molecular mass.

HSV-1-infected cells have previously been shown to encode proteins that bind hIgG but not rodent IgG (39). To investigate the binding characteristics of soluble gE, gI, and the gE-gI

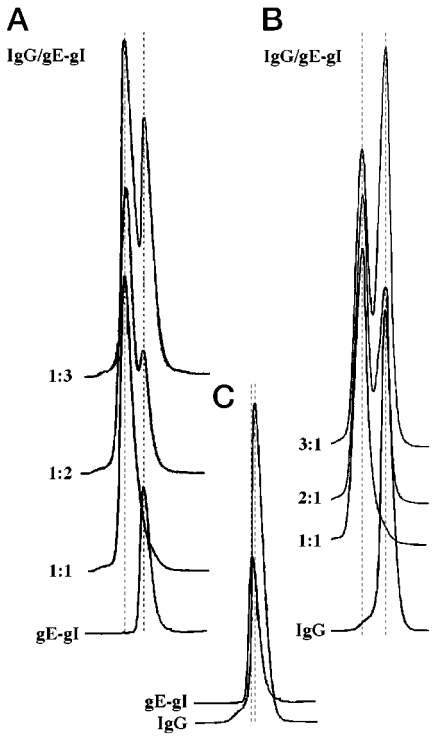

FIG. 2. **Stoichiometry determination of the gE-gI·IgG complex using conventional gel filtration.** gE-gI and IgG were incubated for 30 min at pH 7.4 at the indicated molar ratios and then passed over a size exclusion column to separate the gE-gI·IgG complex from uncomplexed proteins. At a 1:1 molar ratio of gE-gI to IgG, all of the protein chromatographs as a single complex. When the input ratio of gE-gI to IgG is greater than 1:1, there is excess gE-gI (*A*), whereas when the input ratio of IgG to gE-gI is greater than 1:1, there is excess IgG (*B*) (verified by SDS-PAGE analysis; data not shown). *C*, gE-gI and IgG each elute as a single peak and can be distinguished from one another on the basis of their retention times.

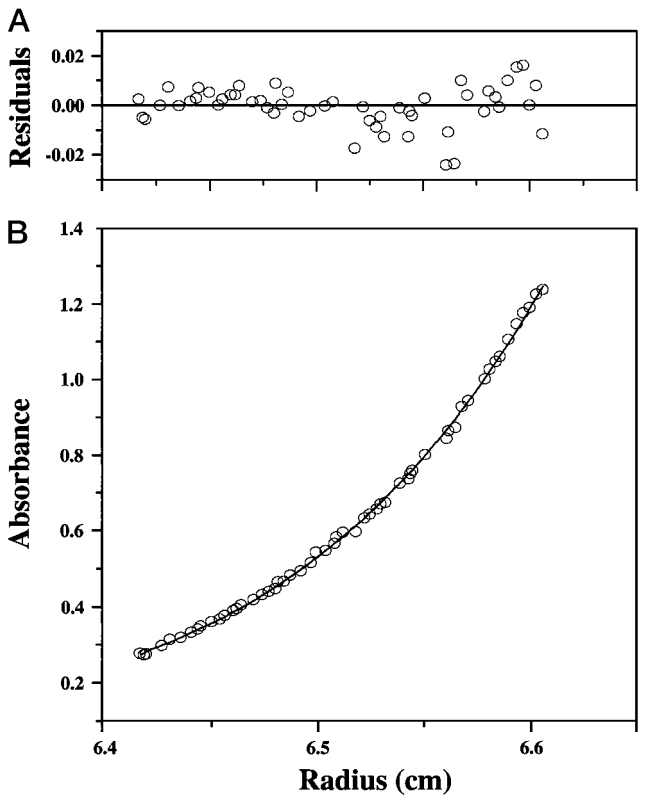

FIG. 3. **Sedimentation equilibrium analysis of gE-gI.** gE-gI at 0.6 mg/ml was centrifuged at 10,000 rpm until equilibrium was reached (36 h). The gradient formed can be best fit to a single species with a mass of 83.4 kDa. The errors of the fit, shown in the residuals plot, are small and random.

heterodimer, metabolically labeled supernatants from gE-, gI-, or gE-gI-secreting cells were incubated with Sepharose-immobilized hIgG or rat IgG. SDS-PAGE analysis revealed that while none of the proteins bind rat IgG, the gE-gI complex efficiently bound to the hIgG matrix. gE alone bound only weakly to the human IgG matrix, while gI alone showed no specific interaction (Fig. 1*B*).

A purification scheme based upon the FcR activity of gE-gI was used to isolate soluble gE-gI heterodimers for biochemical studies. Supernatants from cells expressing gE-gI were passed over an hIgG affinity column, eluted at high pH, and then further fractionated by size exclusion chromatography using a Superose 6B gel filtration column. A single homogenous peak corresponding to a gE-gI complex was obtained, demonstrating that any free gE or gI present in the supernatants does not efficiently associate with the hIgG matrix. By contrast, gE is not purified when supernatants from cells expressing only gE are passed over the hIgG column.

Soluble gE-gI migrates on the gel filtration column slower than predicted by the molecular mass of a 1:1 heterodimer (100 kDa). Indeed, the retention time for gE-gI is greater than that for IgG (165 kDa) (Fig. 2*C*). The increased retention might arise because gE-gI is not a 1:1 heterodimer or because of anomalous migration of a 1:1 heterodimer with an elongated or otherwise nonspherical shape. In order to determine the stoichiometry of soluble gE-gI, we analyzed the protein by N-terminal sequencing and equilibrium analytical ultracentrifugation. N-terminal sequencing of purified gE-gI confirmed the presence of the correctly processed forms of both proteins in approximately stoichiometric amounts (data not shown). The molecular mass of soluble gE-gI determined by equilibrium analytical ultracentrifugation is 83.4 kDa (Fig. 3), in close agreement with the predicted molecular mass of a 1:1 gE-gI heterodimer calculated using molecular masses of each monomer determined by mass spectrometry (gE, 48.4 kDa; gI, 33.5 kDa). To investigate the stability of soluble gE-gI, we used a circular dichroism-based thermal unfolding assay, from which we determined that the heterodimer denatures cooperatively with a T_m of 66 °C (data not shown).

Taken together, these results indicate that gE-gI is a stable heterodimer with 1:1 stoichiometry and that the heterodimer, but neither free gE nor free gI, binds to monomeric hIgG with high affinity. Thus, the observed interaction of free gE with IgG reported here (Fig. 1*B*, *lane 5*) as well as previously (10) must be low affinity or specific for aggregated IgG (11).

The Stoichiometry of the gE-gI·IgG Complex Is 1:1—The stoichiometry of the gE-gI·hIgG complex was determined to be 1:1 using a non-equilibrium-based gel filtration assay and confirmed using an equilibrium column chromatography method (36). As shown in Fig. 2, gE-gI, IgG, and the gE-gI·hIgG complex each elute as single peaks from a Superose 6B column and can be distinguished from one another on the basis of their retention times. To determine the stoichiometry of the gE-gI·IgG complex, various molar ratios of gE-gI to IgG were pre-equilibrated and then passed over the Superose 6B column. When gE-gI and IgG were present at equimolar ratios, a single peak corresponding to the gE-gI·IgG complex eluted from the column (Fig. 2, *A* and *B*). SDS-PAGE analysis of the eluted material revealed that both gE-gI and IgG were present in the peak (data not shown), indicating that gE-gI and IgG form a stable complex under these conditions. When the input ratio of gE-gI to IgG was greater than 1:1, a peak corresponding to excess gE-gI was observed in addition to the gE-gI·IgG complex

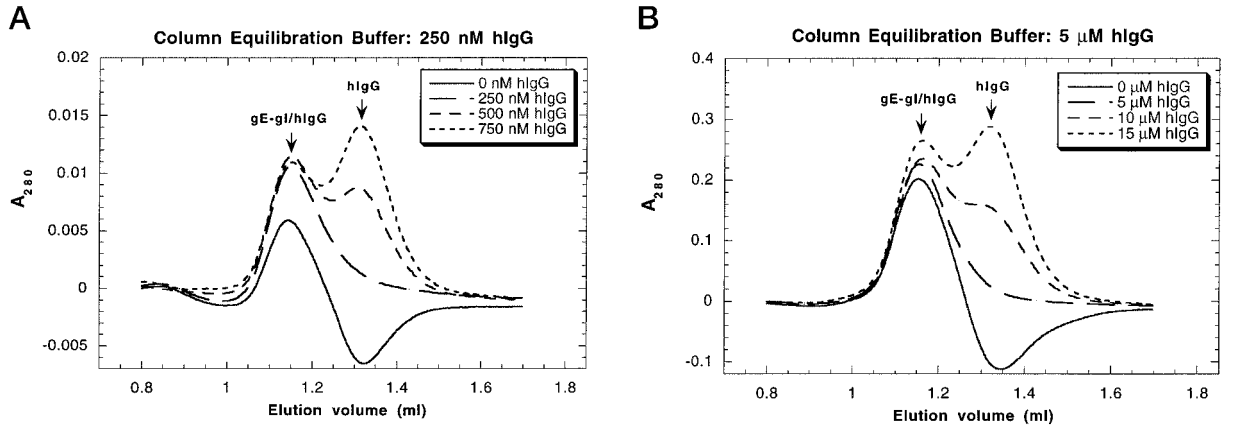

FIG. 4. **Stoichiometry determination of the gE-gI·IgG complex using equilibrium gel filtration.** A Superdex 200 column was equilibrated with 20 mM Tris, 150 mM NaCl, pH 7.4 containing either 250 nM hIgG (*A*) or 5 μM hIgG (*B*). *A*, 250 nM gE-gI was injected in equilibration buffer (20 mM Tris, 150 mM NaCl, pH 7.4, 250 nM hIgG) along with the indicated additional concentrations of hIgG. *B*, 5 μM gE-gI was injected in equilibration buffer (20 mM Tris, 150 mM NaCl, pH 7.4, 5 μM hIgG) along with the indicated additional concentrations of hIgG.

peak, whereas a peak corresponding to excess IgG was observed in addition to the complex peak when the input ratio was less than 1:1 (Fig. 2, *A* and *B*).

To verify the 1:1 stoichiometry of the gE-gI·hIgG complex, we also used an equilibrium-based method. In this method, a gel filtration column was equilibrated with buffer containing a uniform concentration of hIgG (equilibration buffer). gE-gI and hIgG mixtures in equilibration buffer were injected over the gel filtration column. Four injections were made, containing gE-gI at a concentration equal to that of hIgG in the equilibration buffer and either no additional hIgG or 1, 2, or 3 mol eq of hIgG. In all cases, all of the injected gE-gI binds to hIgG, migrating as the gE-gI·IgG complex. When the amount of additional hIgG injected is less than or greater than the amount required for formation of the gE-gI·IgG complex, a trough (in the case of too little hIgG) or a peak (in the case of excess hIgG) should be observed at the position where free hIgG migrates. When the amount of additional hIgG injected is equal to that required for formation of the gE-gI·IgG complex, a flat base line should be observed at the position where hIgG migrates. Over the concentration range from 250 nM (Fig. 4*A*) to 5 μM (Fig. 4*B*), injections of additional hIgG in an amount equivalent to that of gE-gI in the sample result in a flat base line at the hIgG migration position. These results verify that the stoichiometry of the gE-gI·hIgG complex is 1:1 over a protein concentration range of 250 nM to 5 μM.

Residue 435 at the C_H2-C_H3 Domain Interface Is Critical for gE-gI·IgG Binding—Previous IgG binding studies with HSV-1-infected cells indicated that hIgG1, hIgG2, and hIgG4 bind to the HSV-1 FcR, while many hIgG3 allotypes do not bind (39–41). This subtype binding preference resembles the binding preferences for IgG binding by *Staphylococcus aureus* protein A (protein A) and certain classes of rheumatoid factors (RF; antibodies that bind to the Fc portion of Ig) (38, 42–45). We used biosensor-based assays to quantitate the affinity between gE-gI and hIgG subtypes and to characterize the molecular basis of the observed binding specificities. Purified soluble gE-gI was immobilized on the surface of a Biacore biosensor chip using an amine-based coupling chemistry, as described in the Biacore Methods manual. We analyzed the binding of chimeric murine-hIgG molecules composed of the variable domains of a murine anti-dansyl immunoglobulin fused to the constant domains of hIgG1, hIgG2, hIgG3, or hIgG4 (37, 38). The chimeric hIgG subtypes were analyzed for binding to immobilized gE-gI at low coupling densities of gE-gI (100–300 response units), conditions under which mass transport-limited binding is not significant (46). The derived binding constants are summarized in Table I. Chimeric hIgG1, hIgG2, and hIgG4 bind to immobilized gE-gI with equilibrium dissociation constant (K_D) values of 200–400 nM. Of the different hIgG subtypes, hIgG4 has the highest affinity for gE-gI, while hIgG3 does not show detectable binding (>5 response units) at concentrations up to 3.0 μM (Table I and Fig. 5, *A* and *B*).

TABLE I

Binding of hIgG constructs to gE-gI immobilized on a Biacore chip

Kinetic constants were derived from sensorgram data using simultaneous fitting to the association and dissociation curves and global fitting to all curves in a working set. Kinetic analysis was performed using the BIAevaluation version 3.0 package. The equilibrium constants, K_D, were determined from the ratios of the kinetic constants. For hIgG3, hIgG4H435R, and 3–4-3–3, signals of less than 4 RU were observed at protein concentrations of 3.0 μM.

	$k_a \times 10^{-4}$	$k_d \times 10^3$	K_D
	Ms^{-1}	s^{-1}	nM
hIgG1	1.87 ± 0.51	5.09 ± 0.77	282 ± 36
hIgG2	1.96 ± 0.51	6.03 ± 0.08	327 ± 80
hIgG3			
hIgG4	1.75 ± 0.21	3.64 ± 0.44	199 ± 35
hIgG3R435H	1.55 ± 0.44	12.31 ± 4.09	947 ± 533
hIgG4H435R			
3–4-3–3			
3–3-4–4	2.02 ± 0.35	4.66 ± 0.36	240 ± 60
4–3-4–4	1.62 ± 43	2.94 ± 2.04	231 ± 188

For an independent verification of the biosensor-derived affinities, full-length gE and gI were expressed in CHO cells (Fig. 6), and the binding affinity for hIgG4 was derived using iodinated hIgG4. Scatchard analysis of the binding data yields a K_D value of 40.4 ± 13 nM, compared with 199 ± 35 nM in the biosensor-based analysis (Fig. 7). The 5-fold lower affinity determined using the biosensor assay could reflect that covalent immobilization of gE-gI results in reduced affinity for IgG or that the membrane-bound form of gE-gI has a higher affinity for IgG than the soluble version. Although biosensor assays may underestimate the true binding affinity of gE-gI for IgG, they allow quantitative comparison of the relative binding affinities of different hIgG mutants for gE-gI.

Position 435 of hIgG sequences contains a polymorphism that distinguishes many hIgG3 allotypes from hIgG1, hIgG2, and hIgG4. In many hIgG3, residue 435 is an arginine; a histidine is found in all other subclasses. Histidine 435 is a contact residue for protein A binding to IgG Fc (47) and is also important for the binding of some rheumatoid factors to IgG (38, 48, 49). The inability of some RF to recognize hIgG3 can be reversed if the G3m(st) allotype is used. Recognition of this

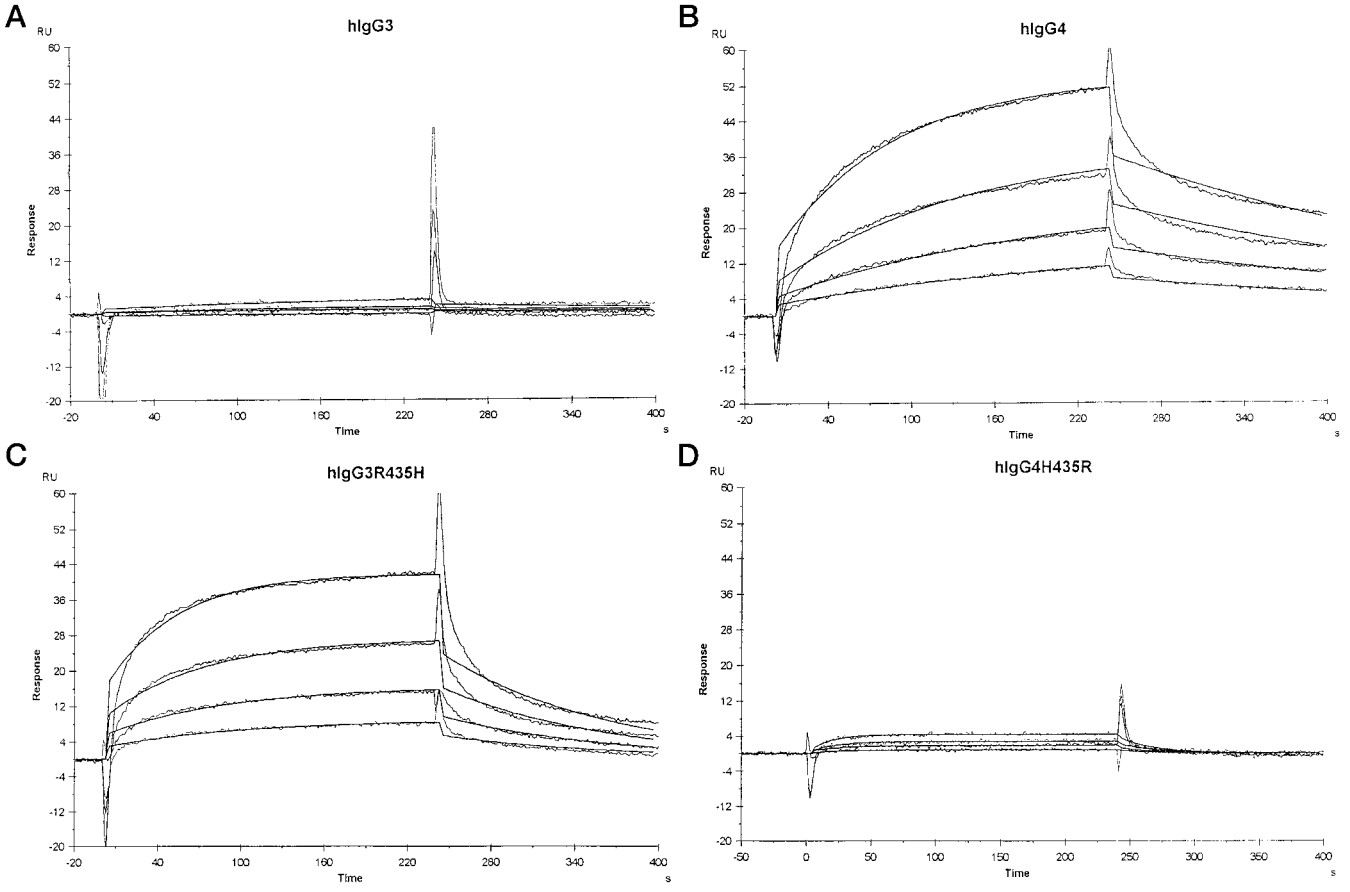

FIG. 5. **Biosensor analysis of the binding of hIgG3, hIgG4, and the corresponding residue 435 mutants.** Soluble gE-gI was immobilized on the surface of a Biacore chip using a primary amine-based coupling protocol. The injected samples were 188 nM to 1.5 μM hIgG3 (*A*), 46–366 nM hIgG4 (*B*), 70.8–566 nM hIgG3R435H (*C*), or 250 nM to 2 μM hIgG4H435R (*D*). For each set of binding experiments, sensorgrams are overlaid with the calculated response using a 1:1 binding model. One representative set of injections from experiments performed in duplicate or triplicate is shown for each interaction.

hIgG3 correlates with the presence of histidine at position 435, while nonbinding hIgG3 have an arginine at position 435 (38, 48). Histidine 435 is located at the interface between the C_H2 and the C_H3 domains of IgG (Fig. 8). The C_H2-C_H3 domain interface of IgG has previously been implicated as the binding site for HSV-1 FcR, based upon inhibition studies with a proteolytic fragment of protein A (50). Alteration of residue 435 could therefore account for the observed differences in gE-gI binding to the hIgG isotypes. Alternatively, since hIgG3 has an extended hinge compared with other hIgG isotypes, hinge-proximal structural differences might account for the observed subtype-specific binding preferences. To investigate these possibilities, we used biosensor assays to examine the binding of gE-gI to mutant hIgG3 and hIgG4 proteins and switch variants in which the constant domains of different subclasses were exchanged by exon shuffling (37, 38).

To investigate the effect of residue 435 upon gE-gI·IgG affinity, the binding of gE-gI to hIgG3 and hIgG4 mutants was examined. The hIgG3 mutant, hIgG3R435H, contains a histidine at residue 435 in place of an arginine in the wild type protein, while the hIgG4 mutant, hIgG4H435R, contains an arginine at residue 435 in place of the histidine in the wild type protein (38). The single residue change of arginine to histidine at residue 435 of hIgG3 is sufficient to restore binding from undetectable in the case of the wild type protein to an affinity of 947 $\pm$ 533 nM in the case of the single site mutant (Fig. 5, *A* and *C*, and Table I). The reciprocal change in hIgG4, histidine to arginine at position 435 (hIgG4H435R), results in no binding at concentrations up to 3 μM, as compared with a binding affinity of 199 $\pm$ 35 nM for wild type hIgG4 (Fig. 5, *B* and *D*, and Table I).

To probe for differences in affinity due to hinge-proximal structural effects, the binding of gE-gI to switch variants of IgG was examined. As described previously, switch variants have been generated by exchanging the constant domains of different subclasses by exon shuffling (38). The switch variants used in these studies were 3-3-4-4 (C_H1 and hinge domains of hIgG3, C_H2, and C_H3 domains of hIgG4), 4-3-4-4 (C_H1, C_H2, and C_H3 domains of hIgG4, hinge of hIgG3), and 3-4-3-3 (C_H1, C_H2, and the C_H3 domains of hIgG3, hinge of hIgG4). Biosensor assays indicate that the switch variants 3-3-4-4 and 4-3-4-4 bind gE-gI with an affinity comparable with that of wild type hIgG4 (Table I). By contrast, the switch variant 3-4-3-3 does not bind at concentrations up to 3.0 μM (Table I). These results demonstrate that histidine 435 at the C_H2-C_H3 domain interface of IgG is critical for gE-gI binding and that the presence of the extended hinge in the chimeric hIgG3 does not significantly hinder binding.

DISCUSSION

We have initiated a molecular characterization of IgG binding by the herpesvirus gE-gI protein. gE and gI are known to associate in HSV-1-infected cells and upon co-expression in heterologous systems (8, 9). Here we show that gE and gI assemble into a stable complex when expressed as soluble proteins. We also show that the soluble gE-gI complex can be purified to homogeneity based upon its Fc receptor function, using IgG affinity chromatography. Gel filtration and analyti-

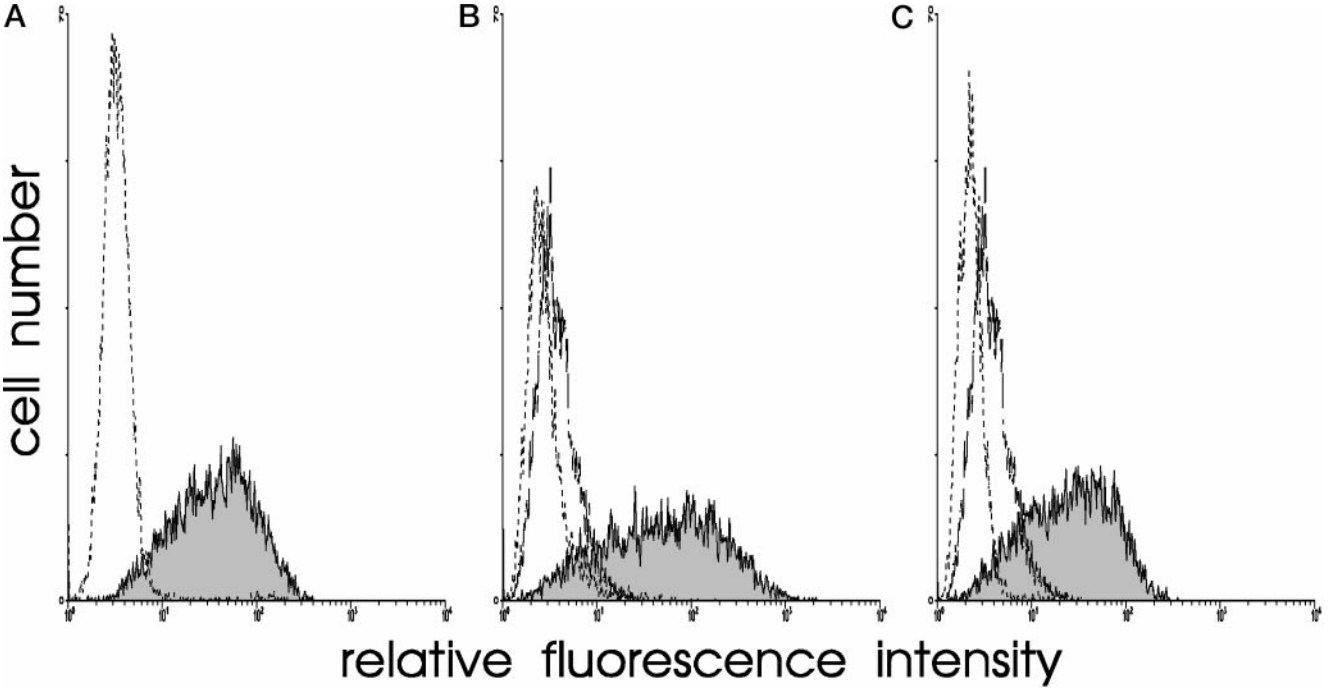

FIG. 6. **Expression of full-length gE and gI in CHO cells.** CHO cells transfected with genes encoding gE and gI were assayed for surface expression of both proteins using flow cytometry. Untransfected (*dotted lines*) or transfected (*solid lines*) cells were stained with FITC-labeled human IgG (*A*), the mouse anti-gE antibody 1108 followed by FITC-labeled goat anti-mouse antibody (*B*), or the mouse anti-gI antibody fd69 followed by FITC-labeled goat anti-mouse antibody (*C*). In *B* and *C*, the *dashed lines* represent staining of transfected cells with FITC-labeled goat anti-mouse antibody alone.

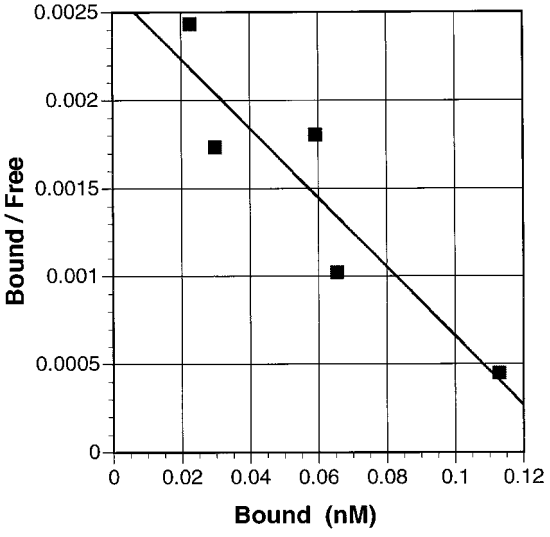

FIG. 7. **Cell binding assay for determination of the binding affinity of membrane-bound gE-gI for IgG.** 1×10^6 CHO cells expressing membrane-bound gE-gI were incubated with different concentrations of ^{125}I-labeled chimeric hIgG4. Binding data are presented as a Scatchard plot. Each point represents the average of two duplicate measurements. Three independent experiments yielded an average binding constant of 40 ± 13 nM.

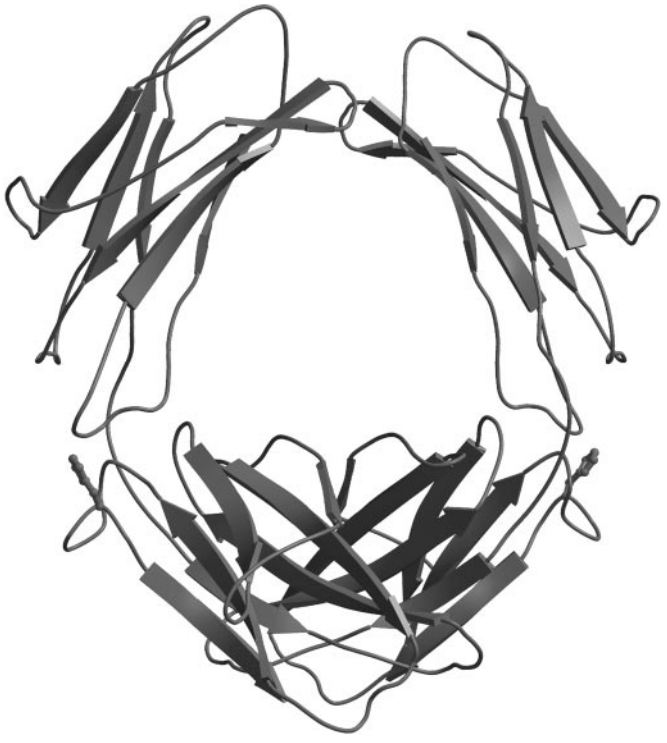

FIG. 8. **The location of histidine 435 on the structure of human Fc.** A *ribbon diagram* of the C_H2 and C_H3 domains of hIgG are shown (47). The side chain of histidine 435 is shown on the carbon-α backbone. The *figure* was prepared using Molscript (75) and rendered using Raster 3D (76).

cal ultracentrifugation experiments establish that soluble gE-gI is a 1:1 heterodimer, consistent with observations for gE-gI complexes derived from other α-herpesviruses (*e.g.* varicella zoster virus (51)). These results demonstrate that the transmembrane and cytoplasmic domains of gE and gI are not required for gE-gI heterodimer assembly and that the extracellular domains are sufficient for the assembly of gE and gI into a stable heterodimer.

Whereas neither gE nor gI alone efficiently bind monomeric hIgG, the gE-gI heterodimer binds hIgG with relatively high affinity. Biosensor-based studies using immobilized gE-gI show that soluble gE-gI binds to hIgG1, hIgG2, and hIgG4 with affinities in the range of 200–400 nM. Results from binding assays using CHO cells expressing membrane-bound gE-gI are in close agreement with the binding constant of 50 nM reported

for the interaction of rabbit IgG with HSV-1-infected cells (52). In addition, the observed binding specificities for the gE-gI interaction with different hIgG subclasses and rodent IgG parallels the binding specificities reported for IgG interaction with HSV-1-infected cells (39, 53). Thus, our results confirm that the FcR activity induced by HSV-1 infection of cells corresponds to IgG binding by cell surface gE-gI heterodimers. The relatively high affinity interaction between gE-gI and the hIgG subtypes 1, 2, and 4 indicates that nonimmune monomeric hIgG can coat HSV-1 virions at the high concentrations of hIgG present in serum (60–70 μM), thereby inhibiting virus neutralization by antiviral antibodies.

Antibody bipolar bridging by gE-gI on HSV-1-infected cells has been implicated in inhibition of ADCC mediated by mammalian FcγRs (20). Human peripheral blood mononuclear cells have been shown to mediate lower levels of ADCC activity against target cells infected with wild type HSV-1 compared with cells infected with a gE-negative HSV-1. These differences were attributed to the engagement of the Fc regions of cell surface-associated antibodies by cognate gE-gI rather than by the FcγR present on opposing immune effector cells. Among mammalian receptors, FcγRI (K_D $\sim 0.5 \times 10^{-9}$ M) is a high affinity receptor, and FcγRII and FcγRIII ($K_D < 1 \times 10^{-6}$ M) are low affinity receptors (reviewed in Refs. 54 and 55). Thus, based upon affinity considerations alone, the formation of a gE-gI·IgG complex is likely to inhibit ADCC mediated by FcγRII and FcγRIII. In addition, the observed 1:1 stoichiometry for IgG interaction with gE-gI, FcγRI, and FcγRIII, as well as the fact that only one of two available binding sites on IgG is a high affinity site in the FcRn-IgG complex (reviewed in Refs. 54 and 55), suggests a marked asymmetry in the Fc regions of receptor-bound IgGs, such that only one of the binding sites is in an optimal conformation for binding to many receptors. The observed 1:1 stoichiometry of the gE-gI·IgG complex at micromolar concentrations of the proteins indicates that the asymmetry of the gE-gI·IgG complex may prevent high affinity interaction with a second gE-gI molecule. Similar mechanisms could also account for a reduced reactivity of the gE-gI·IgG complex with other Fcγ binding proteins, irrespective of the binding site location.

The 1:1 stoichiometry of the gE-gI·IgG complex could have implications for signaling mediated by IgG binding to cell surface gE-gI. Specifically, binding of monomeric IgG would not be expected to induce dimerization of gE-gI heterodimers. However, aggregated IgG (such as IgG in immune complexes) or anti-gE and anti-gI antibodies could result in gE-gI multimerization. In addition, IgG involved in antibody bipolar bridging (21) could result in the oligomerization of gE-gI with other viral glycoproteins. A conserved Y*XX*(L/V) motif is observed in the cytoplasmic domains of gE from HSV-1, HSV-2, and PRV (33, 56, 57). In mammalian receptors, the Y*XX*(V/L) motif is responsible for various signaling events such as the internalization of endocytic receptors from the plasma membrane, protein targeting to various cellular compartments (58), mediation of immune cell activation (59), and inhibition of cellular immune responses (60). The importance of the Y*XX*L motif in mammalian immune responses raises the question of whether the gE-encoded Y*XX*L motif is functional in signal transduction mediated by Fc binding. The FcR activity of gE-gI has been suggested to initiate signaling events that facilitate capping and extrusion of PRV glycoproteins, induced by a polyclonal mixture of porcine anti-PRV antibodies (13). Whether anti-HSV antibodies can mediate glycoprotein capping and extrusion in HSV-infected cells remains an important question to be addressed. If antibody-induced capping and extrusion of viral glycoproteins occurs in HSV-1-infected cells, the importance of Fc binding by gE-gI for the occurrence of the process can be rigorously investigated with the current knowledge of gE-gI binding specificities for different IgG and the interaction stoichiometry. These studies will allow a better understanding of the mechanisms by which the FcR activity of α-herpesviruses could modify the protective effects of antiviral antibodies.

Antibody bipolar bridging has been implicated in inhibition of ADCC by HSV (20) as well as in anti-PRV antibody-mediated glycoprotein capping and extrusion (13); but is antibody bipolar bridging sterically probable? Can an IgG molecule simultaneously use its Fab and the Fc regions in interactions with antigens and Fc receptors? Although direct evidence for the occurrence of antibody bipolar bridging is lacking, fluorescence energy transfer studies indicate that the IgG molecule is highly flexible (61), suggesting that simultaneous interactions of the Fab and Fc domains as postulated in antibody bipolar bridging are feasible.

Using mutant forms of hIgG, we show that histidine 435 at the interface between the C_H2 and C_H3 domains of IgG is critical for the binding interaction. Other proteins known to interact at the C_H2-C_H3 domain interface include protein A (47), protein G (62), the neonatal Fc receptor (63), and RF (44). Crystal structures have been reported for Fc complexes with protein A (47), protein G (64), neonatal Fc receptor (65), and a Fab fragment derived from a human IgM RF antibody (RF-AN) (49, 66). From comparisons of the binding characteristics observed for the gE-gI·IgG complex and IgG complexes with protein A, protein G, neonatal Fc receptor, and RF, it appears that the gE-gI·IgG complex most closely resembles IgG complexes with certain rheumatoid factors. The similarities include a lack of binding of several hIgG3 allotypes, the species specificity (binding to human and rabbit IgG, but lack of binding of rodent IgG (39, 53, 66)), and the importance of histidine 435 in the binding interaction. That the IgG binding specificity of gE-gI closely resembles that of some RF is significant in understanding the origin of RF, since it has been suggested that some RF arise as anti-idiotypic antibodies against antibodies to bacterial or viral Fcγ-binding proteins, in a process known as idiotypic networking (44, 67, 68).

Anti-idiotypic antibodies recognize the idiotypic determinants expressed in the V region of a particular antibody or the V regions of a group of related antibodies. It has been proposed that anti-idiotypic antibodies are expressed in order to regulate the expression of antibodies that dominate the response to a particular antigen (69). Suppression of B cells expressing these dominant antibodies would allow for the proliferation of other antibodies using alternative V region sequences and ultimately to the diversification of the antibody response (70). While the expression of anti-idiotypic antibodies would normally decline with the decreased expression of the antibodies to which they are responding, anti-idiotypic antibodies that cross-react with something so ubiquitous as self-IgG have the potential to be continually propagated. This model of idiotypic suppression provides a possible explanation for the production of RF as a result of HSV-1 infection. Expression of gE-gI on the virion and on the surface of HSV-1-infected cells would lead to production of anti-gE-gI antibodies and subsequently to the production of anti-anti-gE-gI antibodies that have the potential to be RF if the epitope recognized by the anti-gE-gI antibody is the region on gE-gI that interacts with IgG-Fc. In addition, persistence of HSV-I infection may lead to continual production of RF.

The similarities we observe between the gE-gI·IgG complex and IgG complexes with certain classes of RF support the hypothesis that some RF might be anti-idiotypic antibodies against antibodies to gE-gI and provide the basis to more closely examine the linkage between herpesviral infections and

pathogenic RF production. Further support comes from studies by Tsuchiya *et al.* (71), which show that some RF share idiotypic determinants with gE-gI, suggesting that these RF may be anti-idiotypic antibodies against antibodies to gE-gI. However, whether the observed similarities in binding characteristics of gE-gI·IgG and the RF-IgG complexes will correspond to similarities in the interactions at the atomic level remains to be determined from crystallographic comparisons of gE-gI·IgG with RF·IgG complexes that show the closest resemblance in binding characteristics.

Recent studies suggest that antibodies are highly protective against herpes infections in human neonates (72). Based upon the binding studies reported here and previous studies with HSV-1-infected cells (39, 40, 53), gE-gI can mitigate the effects of antiviral antibodies of the IgG1, IgG2, and IgG4 subtypes, whereas IgG3 allotypes might confer the greatest protection to a host due to the inability of many IgG3 allotypes to bind gE-gI. HSV-specific antibodies of the IgG1, IgG3, and IgG4 subclasses have been detected in genital herpes infections (73). Because human neonatal Fc receptor (the receptor responsible for transplacental IgG transfer (74)) binds the four human IgG isotypes with similar affinities,[2] IgG3 is likely to be transferred to the fetus with equal efficacy compared with the other isotypes that are generated, and it may constitute the isotype that confers the greatest protection against neonatal herpes. However, it is possible that anti-HSV hIgG3 antibodies are not produced or are not effective in certain HSV infections, and therefore, a virus expressing an IgG3-binding FcR would not experience a selective advantage. This may explain the lack of hIgG3 binding to gE-gI and the evolution of the viral FcR with specificity for other hIgG subclasses.

Acknowledgments—We thank Philip E. Lapinski for doing the cell binding experiments, the flow cytometry core at the University of Michigan for performing the fluorescence-activated cell sorting analyses, the Reproductive Sciences program at the University of Michigan for IgG radiolabeling, Parke-Davis research facility for use of the Biacore for initial characterization of the gE-gI·IgG complex, and the California Institute of Technology Protein/Peptide Micro Analytical Laboratory for protein analysis. We also thank Pak Poon for doing the equilibrium analytical ultracentrifugation experiments. We thank Dr. Oveta J. Fuller and Pak Poon for many helpful discussions.

REFERENCES

1. Gooding, L. R. (1992) *Cell* **71,** 5–7
2. Banks, T. A., and Rouse, B. T. (1992) *Clin. Infect. Dis.* **14,** 933–941
3. Ploegh, H. (1998) *Science* **280,** 248–253
4. Dubin, G., Fishman, N. O., Eisenberg, R. J., Cohen, G. H., and Friedman, H. M. (1992) *Curr. Top. Microbiol.* **179,** 111–120
5. Westmoreland, D., and Watkins, J. F. (1974) *J. Gen. Virol.* **24,** 167–178
6. Baucke, R. B., and Spear, P. G. (1979) *J. Virol.* **32,** 779–789
7. Para, M. F., Baucke, R. B., and Spear, P. (1980) *J. Virol.* **34,** 512–520
8. Johnson, D. C., and Feenstra, V. (1987) *J. Virol.* **61,** 2208–2216
9. Johnson, D. C., Frame, M., Ligas, M. W., Cross, A. M., and Stow, N. D. (1988) *J. Virol.* **62,** 1347–1354
10. Bell, S., Cranage, M., Borysiewicz, L., and Minson, T. (1990) *J. Virol.* **64,** 2181–2186
11. Dubin, G., Frank, I., and Friedman, H. M. (1990) *J. Virol.* **64,** 2725–2731
12. Hanke, T., Graham, F. L., Lulitanond, V., and Johnson, D. C. (1990) *Virology* **177,** 437–444
13. Favoreel, H. W., Nauwynck, H. J., Van Oostveldt, P., Mettenleiter, T. C., and Pensaert, M. B. (1997) *J. Virol.* **71,** 8254–8261
14. Litwin, V., Jackson, W., and Grose, C. (1992) *J. Virol.* **66,** 3643–3651
15. Nagashunmugam, T., Lubinski, J., Wang, L., Goldstein, L. T., Weeks, B. S., Sundaresan, P., Kang, E. H., Dubin, G., and Friedman, H. M. (1998) *J. Virol.* **72,** 5351–5359
16. Lehner, T., Wilton, J. M. A., and Shillitoe, E. J. (1975) *Lancet* **ii,** 60–62
17. Costa, J. C., and Rabson, A. S. (1975) *Lancet* **i,** 77–78
18. Adler, R., Glorioso, J. C., Cossman, J., and Levine, M. (1978) *Infect. Immun.* **21,** 442–447
19. Dowler, K. W., and Veltri, R. W. (1984) *J. Med. Virol.* **13,** 251–259
20. Dubin, G., Socolof, E., Frank, I., and Friedman, H. M. (1991) *J. Virol.* **65,** 7046–7050
21. Frank, I., and Friedman, H. M. (1989) *J. Virol.* **63,** 4479–4488
22. Whealy, M. E., Card, J. P., Robbins, A. K., Dubin, J. R., Rziha, H.-J., and Enquist, L. W. (1993) *J. Virol.* **67,** 3786–3797
23. Tirabassi, R. S., Townley, R. A., Eldridge, M. G., and Enquist, L. W. (1997) *J. Virol.* **71,** 6455–6464
24. Dingwell, K. S., Brunetti, C. R., Hendricks, R. L., Tang, Q., Tang, M., Rainbow, A. J., and Johnson, D. C. (1994) *J. Virol.* **68,** 834–835
25. Dingwell, K. S., Doering, L. C., and Johnson, D. C. (1995) *J. Virol.* **69,** 7087–7098
26. Balan, P., Davis-Poynter, N., Bell, S., Atkinson, H., Browne, H., and Minson, T. (1994) *J. Gen. Virol.* **75,** 1245–1258
27. Sambrook, J., Fritsch, E. F., and Maniatis, T. (1989) *Molecular Cloning: A Laboratory Manual*, 2nd Ed., Cold Spring Harbor Laboratory, Cold Spring Harbor, NY
28. Gastinel, L. N., Simister, N. E., and Bjorkman, P. J. (1992) *Proc. Natl. Acad. Sci. U. S. A.* **89,** 638–642
29. Bebbington, C. R., and Hentschel, C. C. G. (1987) in *DNA Cloning: A Practical Approach* (Glover, D. M., ed) pp. 163–188, IRL Press, Oxford
30. Metcalf, J. F., Chatterjee, S., Koga, J., and Whitley, R. J. (1988) *Intervirology* **29,** 39–49
31. Longnecker, R., Chatterjee, S., Whitley, R. J., and Roizman, B. (1987) *Proc. Natl. Acad. Sci. U. S. A.* **84,** 4303–4307
32. Harlow, E., and Lane, D., *Antibodies: A Laboratory Manual* (1988) *Antibodies: A Laboratory Manual*, pp. 310–311, Cold Spring Harbor Laboratory, Cold Spring Harbor, NY
33. McGeoch, D. J., Dolan, A., Donald, S., and Brauer, D. H. (1985) *J. Mol. Biol.* **181,** 1–13
34. Gill, S. C., and Von Hippel, P. H. (1989) *Anal. Biochem.* **182,** 319–326
35. Zamyatnin, A. A. (1972) *Prog. Biophys. Mol. Biol.* **24,** 107–123
36. Hummel, J. P., and Dreyer, W. J. (1962) *Biochim. Biophys. Acta* **63,** 530–532
37. Artandi, S. E., Canfield, S. M., Tao, M., Calame, K. L., Morrison, S. L., and Bonagura, V. R. (1991) *J. Immunol.* **146,** 603–610
38. Bonagura, V. R., Artandi, S. E., Agostino, N., Tao, M., and Morrison, S. L. (1992) *DNA Cell Biol.* **11,** 245–252
39. Johansson, P. J., Myhre, E. B., and Blomberg, J. (1985) *J. Virol.* **56,** 489–494
40. Wiger, D., and Michaelsen, T. E. (1985) *Immunology* **54,** 565–573
41. Johansson, P. J., Ota, T., Tsuchiya, N., Malone, C. C., and Williams, R. C. (1994) *Immunology* **83,** 631–638
42. Kronvall, G., and Williams, R. C. (1966) *J. Immunol.* **103,** 828–833
43. Allen, J. C., and Kunkel, H. G. (1966) *Arthritis Rheum.* **9,** 758–768
44. Nardella, F. A., Teller, D. C., Barber, C. V., and Mannik, M. (1985) *J. Exp. Med.* **162,** 1811–1824
45. Langone, J. J. (1982) *Adv. Immunol.* **32,** 157–252
46. Karlsson, R., and Falt, A. (1997) *J. Immunol. Methods* **200,** 121–123
47. Deisenhofer, J. (1981) *Biochemistry* **20,** 2361–2370
48. Bonagura, V. R., Artandi, S. E., Davidson, A., Randen, I., Agostino, N., Thompson, K., Natvig, J. B., and Morrison, S. L. (1993) *J. Immunol.* **151,** 3840–3852
49. Sutton, B. J., Corper, A. L., Sohi, M. K., Beale, D., and Taussig, M. J. (1998) *Adv. Exp. Med. Biol.* **435,** 41–50
50. Johansson, P. J., Nardella, F. A., Sjöquist, J., Schröder, A. K., and Christensen, P. (1989) *Immunology* **66,** 8–13
51. Kimura, H., Straus, S. E., and Williams, R. K. (1997) *Virology* **233,** 382–391
52. Johansson, P. J., and Blomberg, J. (1990) *APMIS* **98,** 685–694
53. Johansson, P. J., Hallberg, T., Oxelius, V. A., Grubb, A., and Blomberg, J. (1984) *J. Virol.* **50,** 796–804
54. Hulett, M. D., and Hogarth, P. M. (1994) *Adv. Immunol.* **57,** 1–127
55. Raghavan, M., and Bjorkman, P. (1996) *Annu. Rev. Cell Dev. Biol.* **12,** 181–220
56. Petrovskis, E. A., Timmins, J. G., and Post, L. E. (1986) *J. Virol.* **60,** 185–193
57. McGeoch, D. J., Moss, H. W., McNab, D., and Frame, M. C. (1987) *J. Gen. Virol.* **68,** 19–38
58. Trowbridge, I. S., Collawn, J. F., and Hopkins, C. R. (1993) *Annu. Rev. Cell Biol.* **9,** 129–161
59. Cambier, J. C. (1992) *Curr. Opin. Immunol.* **4,** 257–264
60. Leisbon, P. J. (1997) *Immunity* **6,** 655–661
61. Zheng, Y., Shopes, B., Holowka, D., and Baird, B. (1992) *Biochemistry* **31,** 7446–7456
62. Stone, G. C., Sjöbring, U., Björck, L., Sjöquist, J., Barber, C. V., and Nardella, F. A. (1989) *J. Immunol.* **143,** 565–570
63. Raghavan, M., Chen, M. Y., Gastinel, L. N., and Bjorkman, P. J. (1994) *Immunity* **1,** 303–315
64. Sauer-Eriksson, A. E., Kleywegt, G. J., Uhlen, M., and Jones, T. A. (1995) *Structure* **3,** 265–278
65. Burmeister, W. P., Huber, A. H., and Bjorkman, P. J. (1994) *Nature* **372,** 379–383
66. Corper, A. L., Sohi, M. K., Bonagura, V., Steinitz, M., Jefferis, R., Feinstein, A., Beale, D., Taussig, M. J., and Sutton, B. J. (1997) *Nat. Struct. Biol.* **4,** 374–381
67. Cooke, A., Lydyard, A. M., and Roitt, I. M. (1984) *Lancet* **2,** 723–725
68. Plotz, P. H. (1983) *Lancet* **2,** 824–826
69. Jerne, N. K. (1974) *Ann. Immunol.* (*Paris*) **125C,** 373–389
70. Lange, H., Solterback, M., Berek, C., and Lemke, H. (1996) *Eur. J. Immunol.* **26,** 2234–2242
71. Tsuchiya, N., Williams, R. C., and Hutt-Fletcher, L. M. (1990) *J. Immunol.* **144,** 4742–4748
72. Brown, Z. A., Selke, S., Zeh, J., Kopelman, J., Maslow, A., Ashley, R. L., Watts, M. D., Berry, S., Herd, M., and Corey, L. (1997) *N. Engl. J. Med.* **337,** 509–515
73. Hashido, M., and Kawana, T. (1997) *Microbiol. Immunol.* **41,** 415–420
74. Story, C. M., Mikulska, J. E., and Simister, N. E. (1994) *J. Exp. Med.* **180,** 2377–2381
75. Kraulis, P. J. (1991) *J. Appl. Crystallogr.* **24,** 946–950
76. Merritt, E. A., and Murphy, M. E. P. (1994) *Acta Crystallogr. Ser. D.* **50,** 869–873

[2] A. P. West and P. J. Bjorkman, unpublished results.